
Article:
Haque, N, Jegede, OE and Mullis, AM orcid.org/0000-0002-5215-9959 (2021) The Development of Plate and Lath Morphology in Ni_5Ge_3. Physics of Metals and Metallography, 122 (14). pp. 1537-1542. ISSN 0031-918X

https://doi.org/10.1134/S0031918X21140106

The development of plate and lath morphology in Ni_5Ge_3

N. Haque [a, b], O. E. Jegede [a], A. M. Mullis [a]

[a] *School of Chemical & Process Engineering, University of Leeds, Leeds LS2 9JT, UK*
[b] *Department of Metallurgical Engineering, NEDUET, University Road, Karachi 75270, Pakistan*
e-mail: engrnafis@gmail.com, Phone number: 00923002375065

Drop-tube processing was used to solidify rapidly a congruently melting, single phase intermetallic Ni_5Ge_3. This process results in the production of powders with diameters that are between 850 – 53 μm. After etching that occurs at low cooling rates (850 – 150 μm diameter particles, 700 – 7800 K s^{-1}), an isolated plate and lath microstructure in what is an otherwise featureless matrix constitutes the dominant solidification morphology. By contrast, when the cooling rates are higher (150 – 53 μm diameter particles, 7800 – 42000 K s^{-1}), it is isolated hexagonal crystallites within a featureless matrix, which constitute the dominant solidification morphology. The TEM analysis of selected area diffraction shows that plate and lath microstructures are variants of ε-Ni_5Ge_3, which are partially ordered. By contrast, the isolated hexagonal crystallites are revealed to be disordered. However, the featureless matrix of both microstructures are the fully ordered variant of the same compound. The plate & lath has a very different EBSD and GOS signatures to the hexagonal crystallites structure. Histogram of the correlated grain orientation angle distribution across grain orientation in plate & lath microstructure sample from the 300 – 212 μm fraction showing predominance of low angle grain boundaries. However, grain orientation in isolated hexagonal crystallites from 150 – 106 μm revealing the distribution typical of random grain orientation.

Keywords: rapid solidification, intermetallic compound, plate & lath microstructure, isolated hexagonal crystallites.

INTRODUCTION

Intermetallic compounds such as Ti_3Al have received considerable attention since the 70's due to their potential as structural material for high temperature applications. Ti_3Al is characterised by a high elastic modulus, low density and good mechanical properties at elevated temperature, together with good oxidation resistance. Furthermore, these intermetallic alloys display good dimensional stability [1] and, in contrast to ceramics, can display good ductility at room temperature with appropriate processing. Additionally, they exhibit good thermal conductivity. For these reasons, Ti_3Al has been the object of much attention as a high temperature structural material for aerospace application [2, 3] such as in compressor rotors and afterburner nozzles [3]. Ti_3Al is also used commercially in the automotive industry, where applications include turbo-fan rotors and exhaust valves [4]. The purpose of this study is to examine, using drop-tube processing, the solidification morphologies, which are connected to high growth rate disorder trapping. Despite its commercial importance, there have been few systematic studies to date of order-disorder reactions in Ti_3Al. [5-7]. The high chemical reactivity of Ti_3Al melt favours easy heterogeneous nucleation thereby suppressing undercooling during normal material processing. However, recently [8] have succeeded in obtaining high undercooling in Ti_3Al melts using electromagnetic levitation techniques.

An alternative approach is the use of an analogue system, crystallographically similar to Ti_3Al but which is easier to process. One such is the congruently melting intermetallic compound Ni_5Ge_3 which shares the $P6_3/mmc$ crystal structure with Ti_3Al. Moreover, congruently melting compounds are particularly well suited to studying the effects of disorder trapping in intermetallics in that, with the melt at the stoichiometric composition, solidification occurs without partitioning of solute, even during equilibrium solidification. Consequently, it is possible to study disorder trapping without having to consider simultaneous solute trapping, which would otherwise complicate the interpretation of results.

In this study, rapidly solidified Ni-37.2 at%. Ge, are examined and presented, which is close to the stoichiometry of the Ni_5Ge_3. The drop tube process, in which cooling rate is first set-on through powder size, impacts on rapid solidification. The key objective of this work is established on the examination of EBSD consequences of the rapidly solidified Ni_5Ge_3 compound. In this study two dissimilar microstructures were found namely, plate & lath

structure and isolated faceted hexagonal crystallites. Where, at low cooling rates such as 700 – 7800 K s^{-1} within the sample size 850 – 150 µm, produced plate & lath structure. However, at higher cooling rates such as 7800 – 42000 K s^{-1} within the sample size 150 – 53 µm, isolated faceted hexagonal crystallites were observed.

EXPERIMENTAL METHODS

The congruently melting ε-Ni5Ge3 compound occurs over the homogeneity range of 33.6 to 42.2 at. % Ge. ε-Ni5Ge3 and has the ordered hexagonal P63/mmc crystal structure [9]. ε-Ni5Ge3 was made via arc-melting Nickel and Germanium composed in a protective argon (Ar) atmosphere. XRD analysis using a PANalytical Xpert Pro X-Ray diffractometer to verify the phase composition of the subsequent ingot.

In this research work, a 6.5 m drop-tube was used for rapid solidification process. The arc melted sample of ε-Ni5Ge3, 9.4 g mass was loaded into an alumina crucible. At the bottom of this crucible has three 300 µm laser drilled holes. The arc-melted sample heated/melted by induction melting system. The pressuring of the crucible with 400 kPa of N2 gas led to the melt being ejected at a crucible temperature of 1533 K/1260 °C (75 K superheat). From this a fine spray of droplets are produced, which become solid in-flight. These droplets are at the base of the tube. The drop-tube method is explained in detail in [10]. Ten different size of samples ranges between ≥ 850 µm (< 700 K s-1) to ≤ 38 µm (> 54500 K s-1) were obtained subsequent evacuation from the drop tube. The methodology for calculation of cooling rate for the each size fraction are described in [11].

In this paper we present our results for the 850 - 53 µm drop-tube samples. XRD analysis was performed on the drop-tube powders in order to check that the material stayed single phase subsequent processing. Following this drop-tube the powders were mounted and polished to a 1 µm surface finish for microstructural analysis. A 0.1 µm colloidal silica suspension was used to obtain the high quality surface finish required for EBSD analysis. A Carl Zeiss EVO MA15 scanning electron microscope (SEM) was used for metallographic analysis. A combination of equivalent portions HF, HCl and HNO3 was used to perform the etching of samples. In order to identify the chemical homogeneity of samples, an Oxford Instrument X-Max Energy-Dispersive X-Ray (EDX) detector was utilised. A FEI Quanta 650 FEGSEM with Oxford/HKL Nordlys EBSD system was used to perform Electron Back-Scatter Diffraction (EBSD) on unetched samples.

RESULTS AND DISCUSSION

Samples of the intermetallic compound ε-Ni5Ge3 were rapidly solidified from their parent melt using a drop-tube technique. XRD analysis confirmed that starting material/arc-melted sample for the drop-tube experiments is ε-Ni5Ge3, single-phase. In Figure 1, it is shown that XRD peaks may be indexed to ε-Ni5Ge3 by the ICCD reference 04-004-7264. The XRD results in the Figure 1 also show that it is also true with rapid cooling by drop tube (diameter 850 µm to 53 µm).

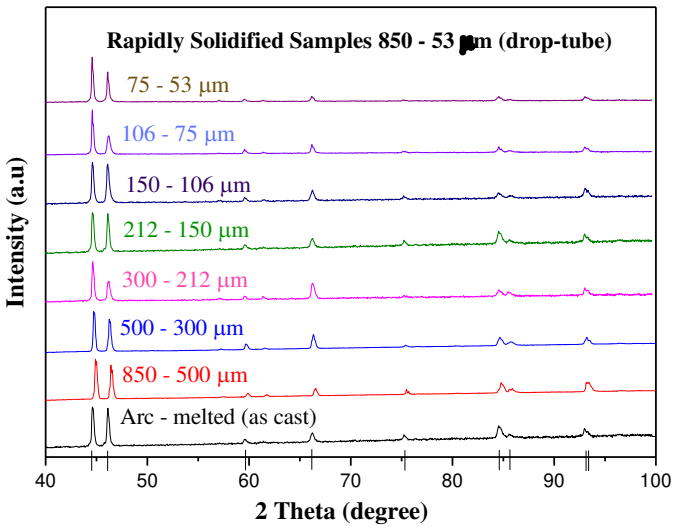

Figure 1: X-ray diffraction analysis of as cast sample preceding to drop tube experiment (black) and rapidly solidified sample (drop tube processed) powder in the 850 – 53 µm size fraction. Vertical black lines indicate peak position for the Ni_5Ge_3 reference pattern.

For the study of microstructure of rapidly solidified Ni_5Ge_3 samples, SEM was used in this work. SEM images of HF etched samples from sieve fractions 850 – 500 µm, 500 – 300 and µm, 300 – 212 µm are shown in the Figures 2 (a-c) respectively, in which many structure like plate & lath can be seen. Note that grain boundaries are also evident and that many of the plate & lath morphologies appear to cross the grain boundaries unaltered. Such structures are the dominant solidification morphology in the drop-tube samples in sieve size fractions ranging from 850 µm to 150 µm. However for particle size smaller than 150 µm, these plate and lath structures are exchanged via numerous isolated faceted hexagonal crystallites with uniformly featureless matrix as can be seen in the Figure 2 (d-f) which show SEM micrographs for the three smallest samples, 150 – 106 µm, 106 – 75 µm, and 75 – 53 µm respectively. In Figure 2f, it also appears that a grain boundary cuts straight through one of the isolated hexagonal crystallites.

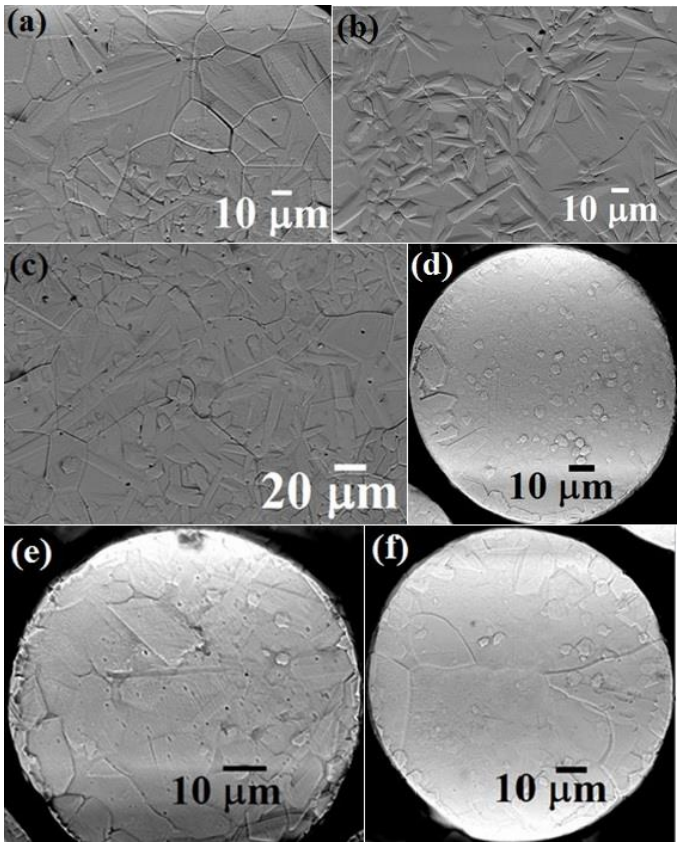

Figure 2: SEM micrograph of HF etched Ni_5Ge_3 drop tube from (a) 850 – 500 μm, (b) 500 –300 μm, and (c) 300 – 212 μm showing numerous plate & lath structures. While, (d) 150 – 106 μm, (e) 106 –75 μm and (f) 75 – 53 μm showing numerous Isolated hexagonal crystallites structrues.

Structures of the plate & lath kind type quite familiar in intermetallic compounds [12-14], and may also be found in some iron alloys [15]. Plate & lath structures found in γ-TiAl [12]. Hyman et al. [12] reported that this resulted from α dendrites transforming in the solid-state during cooling. This transformation led to a mixture of α_2 + γ laths enclosed through γ-segregates. McCullough et al. observed that plate and lath morphologies were also found in α_2-Ti_3Al. Like ε-Ni_5Ge_3, α_2-Ti_3Al shares the P63/mmc space group [13]. Moreover, Popov *et al.* [16] also reported the formation of an ordered Ti_3Al phase (α_2 phase) in Ti–Al alloys. They proposed that the nucleation and growth mechanism involve during formation of particles and the precipitation occurs at temperatures above the ordering temperature. Yet, in materials, such as Ti_3Al, which have the same plate and lath structure, it is the contrast between different phases that gives rise to a different morphology. In contrast, the material being discussed here is single phase (as shown in Figure 1). Moreover, in the case of a congruently melting compound the contrast would not be expected to arise from compositional differences in the as-solidified material. The absence of solute partitioning is established elsewhere [17, 18], where it is shown by EDX line scan across an isolated plate & lath feature [18], that material is chemically homogeneous to within the experimental error related with the technique. This is also the case for the isolated hexagonal crystallites morphology [18], which is similarly shown to be chemically homogeneous across features. As a consequence difference that is the etching process shows seems not to have a relation to either difference in the phases present nor to chemical composition.

In fact, the contrast appears to be due to the extent of chemical ordering displayed by the material. SAD analysis in the TEM shows the isolated hexagonal crystallites, are a disordered variant, while plate and lath microstructure are the partially ordered variant of ε-Ni5Ge3. However, the featureless matrix of both microstructures is the fully ordered variant of the same compound [18]. Such contrast arising due to the preferential etching of the disordered material while the ordered material remains resistant to the etch has been reported in other intermetallic compounds [19, 20]. We show elsewhere that at highest cooling rate (> 42000 K s-1) all material transformed into the disordered variant, often with only a single crystal per droplet [18]. However, at cooling rates < 42000 K s-1 the material has a mixed ordered-disordered structure.

EBSD Euler mapping was used to study the plate & lath and isolated faceted hexagonal crystallite structures within the rapidly solidified droplets. For this, samples were utilised, which were polished without etching and by using 0.1 μm colloidal silica. The EBSD Euler map shows very clearly the grain structures characteristic of the two morphologies are very clearly revealed in the EBSD Euler map, with one example from each morphology (300 – 212 μm, plate and lath) and (150 – 106 μm, isolated hexagonal crystallites) being shown in the Figures 3 a&c respectively. The EBSD Euler map shows no evidence of either the plate and lath nor hexagonal morphologies visible in the EBSD images. This contrasts with the SEM secondary electron images in which a minimum of one plate and lath structure is contained in each grain. In this regard we note that the size of these features, certainly the plate and lath structures should be resolvable by EBSD. We can infer from the non-detection of these microstructural features that were so evident in the etched samples, that their crystallography must be contiguous with the grains in which they are embedded. This is consistent with TEM diffraction analysis, in which sharp diffraction spots are apparent as found previously [17, 18]. The appearance of these spots is consistent with the beam being focused on an area that has a single

crystallographic orientation. As such the results are consistent with the co-existence of disordered and ordered regions within a single grain.

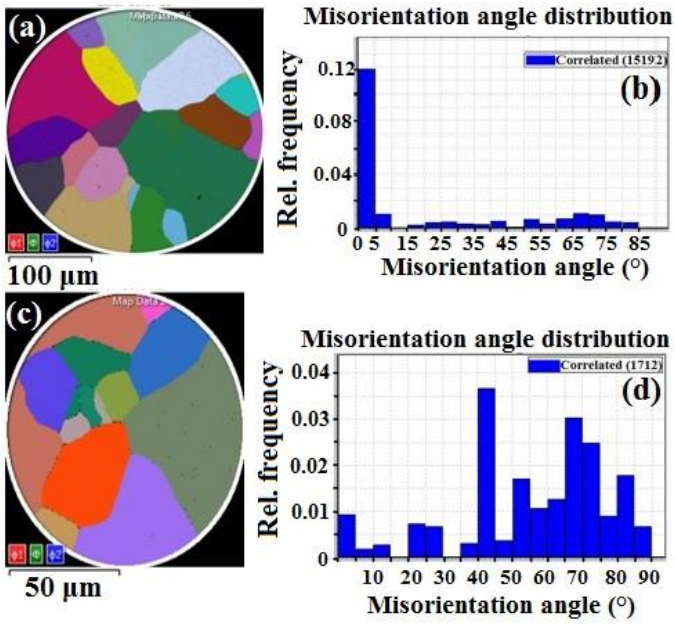

Figure 3 : (a&c) shows EBSD results of Euler texture map of unetched Ni5Ge3 drop-tube particles from the 300 – 212 µm size (plate & lath structure) and 150 – 106 µm size (hexagonal crystallites structure) respectively and (b&d) shows the histogram of the correlated misorientation angle distribution across grain boundaries for the images shown in (a&c).

The plate & lath structure has a very different EBSD signature to that of the hexagonal crystallites. The histogram of grain orientations, 300 – 212 µm sieve fraction (plate & lath microstructure) is pictured in Figure 3b. Figure 3b shows that the majority of grain boundary misorientations are < 10°. This is not the distribution that would be expected due to randomly nucleated grains [21]. The predominance of low angle grain boundaries in the distribution for the 300 – 212 µm particles is suggestive of a structure that has undergone a post solidification modification process. This was not the case for the 150 – 106 µm particles. In fact, in the smaller sieve, the grain orientation distribution of the sample (shown in Figure 3d) is similar to what would be expected from a random population of grains [21].

This also seems to be consistent with the grain orientation spread (GOS) maps for the two samples (see Figure 4 a-b). For the 300 – 212 µm droplets the GOS map shows that most of the grains have a very small GOS, but a small number have a much larger spread (up to 2°). Such GOS distributions are commonly seen in samples having undergone recrystallization and recovery, again suggesting that the sample has undergone some form of post solidification modification. In contrast, the GOS map for the smaller size particles shows a much more uniform spread, but with a larger median value, which would be consistent with this sample having not undergone such modification. Whether this directly accounts for the transition from plate & lath to hexagonal is uncertain as neither structure shows up in EBSD. Nonetheless, it would not be an unreasonable assumption to think that there may be some correlation between the EBSD results which are indicative of some post solidification modification of the structure and the occurrence of the plate & lath morphology.

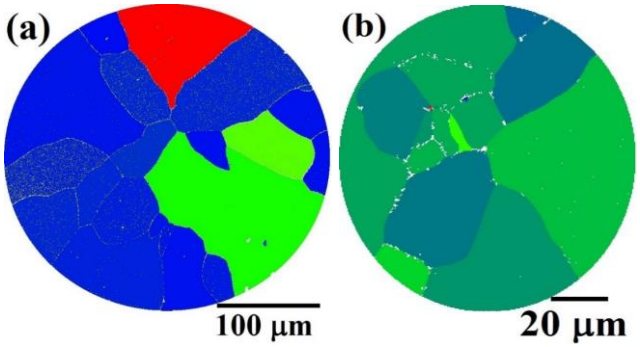

Figure 4: (a&b) shows EBSD results of GOS map of unetched Ni5Ge3 drop tube samples from the 300 – 212 µm size (plate & lath structure) and 150 – 106 µm size (hexagonal crystallites structure) correspondingly.

CONCLUSION

Drop-tube processing has been used to rapidly solidify single phase Ni5Ge3 powders in the size range 850 – 53 µm. The resultant cooling rates is 700 – 42000 K s-1. After etching, two dominant solidification morphologies, plate & lath (850 – 150 µm diameter particles, 700 – 7800 K s-1) and isolated hexagonal crystallites (150 – 53 µm diameter particles, 7800 – 42000 K s-1) are revealed, both of which are embedded within a featureless matrix. The plate & lath structure appears to be the result of a post-solidification modification process. The nature of this process is somewhat unusual as it involves some degree of recrystallization (shown in EBSD) combined with some degree of chemical ordering, which gives the plate and lath morphology. It is presumed that the excess free energy associated with chemical disorder drives the recrystallization process which also results in chemical ordering. In contrast, in the smaller particles, we can postulate that the higher cooling rates suppress the recrystallization part of the transformation, but does not fully suppress the ordering reaction, giving rise to the hexagonal microstructures.

ACKNOWLEDGMENTS

Nafisul Haque is thankful to the Higher Education Commission (HEC) Pakistan and NED University of Engineering & Technology for financial support.

REFERENCES

[1] A. Vasudevan, J. Petrovic, "A comparative overview of molybdenum disilicide composites", Mat. Sci. Eng. A. 1-17, 155 (1992).

[2] D.M. Dimiduk, D. Miracle, C. Ward, "Development of intermetallic materials for aerospace systems", Mater. Sci. Tech. 367-375, 8 (1992).

[3] D. Banerjee, In: Westbrook JH, Fleischer RL (eds) Intermetallic compounds: principles and practice, Intermetallic compounds, Ti_3Al and its alloys, Wiley, New York, 1994.

[4] F.H. Froes, C. Suryanarayana, D. Eliezer, "Synthesis, properties and applications of titanium aluminides", J. Mater. Sci. 5113-5140, , 27 (1992).

[5] C. Liauo, H. Fu, I. Hsiao, J. Huang,"On the β-transus and order/disorder transition temperature in superplastic super α2 Ti_3Al base alloy", Mat. Sci. Eng. A. 275-285, 271 (1999).

[6] Y. Koizumi, H. Katsumura, Y. Minamino, N. Tsuji, J. Lee, H. Mori," Growth kinetics of antiphase domain in Ti_3Al intermetallic compound", Sci. Technol. Adv. Mat. 19-28, , 5 (2004).

[7] T. Radchenko, V. Tatarenko, H. Zapolsky, D. Blavette, "Statistical-thermodynamic description of the order–disorder transformation of D019-type phase in Ti–Al alloy", J Alloy Comp.122-126, 452 (2008).

[8] W. Shao-Lou, H. Lu-Jun, C. Jian, Y. Shang-Jing, G. Lin, "Substantial undercooling and rapid dendrite growth of liquid Ti-Al alloy", Acta. Phys. Sin. 65 (2016).

[9] A. Nash, P. Nash, Binary Alloy Phase Diagrams, in: US National Bureau of Standards Monograph Series 25, Elsevier, ASM, Ohio, 1976, pp. 35.

[10] N. Haque, R.F. Cochrane, A.M. Mullis, "Rapid solidification morphologies in Ni_3Ge: Spherulites, dendrites and dense-branched fractal structures", Intermetallics, 76 (2016) 70-77.

[11] N. Haque, R.F. Cochrane, A.M. Mullis, "The Role of Recrystallization in Spontaneous Grain Refinement of Rapidly Solidified Ni_3Ge", Metall Mater Trans A. 5424-5431, 48 (2017).

[12] M. Hyman, C. McCullough, J. Valencia, C. Levi, R. Mehrabian, "Microstructure evolution in TiAl alloys with B additions: conventional solidification", Metall. Trans. A. 1847 , 20 (1989).

[13] C. McCullough, J. Valencia, C. Levi, R. Mehrabian, "Microstructural analysis of rapidly solidified Ti- Al- X powders", Mat. Sci. Eng. A. 83-101, 124 (1990).

[14] T. Broderick, A. Jackson, H. Jones, F. Froes, "The effect of cooling conditions on the microstructure of rapidly solidified Ti-6Al-4V", Metall Trans A. 1951-1959, , 16 (1985).

[15] G. Krauss, A. Marder, "The morphology of martensite in iron alloys", Metall Mater Trans B. 2343-2357 , 2 (1971).

[16] A. Popov, K. Lugovaya, E. Popova, V. Makarov, M.J.P.o.M. Zhilyakova, Metallography, Features of the Two-Phase ($\alpha+\alpha_2$) Structure Formation in the Ti–17 at% Al alloy, 121 (2020) 791-796.

[17] N. Haque, R.F. Cochrane, A.M. Mullis, "Mechanical Properties of Rapidly Solidified Ni 5 Ge 3 Intermetallic", in: TMS Annual Meeting & Exhibition, Springer, 2018, pp. 705-711.

[18] N. Haque, R.F. Cochrane, A.M. Mullis, "Order-disorder morphologies in rapidly solidified ε/ε′-Ni 5 Ge 3 intermetallic", J Alloy Comp. 327-331, 707 (2017).

[19] N. Haque, R.F. Cochrane, A.M. Mullis, "Morphology of Spherulites in Rapidly Solidified Ni3Ge Droplets", Crystals, 7 (2017) 100.

[20] N. Haque, R.F. Cochrane, A.M. Mullis, "Disorder-order morphologies in drop-tube processed Ni 3 Ge: Dendritic and seaweed growth", J Alloy Comp. 327 - 331, 707 (2017).

[21] J.K. MacKenzie, "The distribution of rotation axes in random aggregate of cubic crystals", Acta Metall. 223-225,12 (1964).